Modeling Fluid Phase Transition Effects on Dynamic Behavior of ESDV

Haroun Mahgerefteh and Pratik Saha
Dept. of Chemical Engineering, University College London, London WC1E 7JE, U.K.

Ioannis G. Economou
Molecular Modelling of Material Laboratory, Institute of Physical Chemistry, National Research Centre for Physical Sciences ''Demokritos,'' GR-15310 Aghia Paraskevi Attikis, Greece

The characteristics method was employed to elucidate the effects of fluid-phase transition on the dynamic behavior of emergency shutdown valves following full bore rupture (FBR) of long pipelines containing high-pressure hydrocarbons. The responses of both check valves and ball valves were simulated. The application of the model to the FBR of the Piper-Alpha MCP-01 gas riser reveals that condensation of the gaseous inventory results in a delay in valve activation times, as well as an increase in the amount of inventory released prior to pipeline isolation. However, the magnitude of the pressure surge brought about from having to bring the high-pressure escaping fluid to rest following emergency isolation was significantly reduced.

Introduction

Huge quantities of highly flammable pressurized hydrocarbons are frequently transported through thousands of kilometers of pipelines across the world. Although this method of transportation is considered to be safe, accidents resulting in pipeline rupture regularly occur (Bond, 1996), and the consequences can be catastrophic both in terms of loss of life and extensive damage to the environment. According to data published by the U.S. Department of Transport (1997), even short, simple pipelines will have a reportable accident during a 20-year lifetime. Operators of long pipelines (1,000 km or over) can expect a reportable accident at a frequency of one per year. Such statistics may well turn out to have enormous financial implications for pipeline operators, as environmental groups in the U.S. are currently pressing for legislation to allow citizens to file lawsuits in federal courts against pipelines which are posing ''imminent and substantial endangerment to health or the environment'' (Barlas, 1999).

According to recent surveys (Hovey and Farmer, 1993; Montiel et al., 1996), the most common causes of pipeline rupture include mechanical failure (such as corrosion), impact failure (excavating machinery and heavy objects), human error, and external events (such as subsidence and sabotage). Pipeline damage on the other hand may be in the form of full bore rupture, a simple puncture, or longitudinal tear. Of these, full bore rupture (FBR), in which the pipeline is split into two across its circumference, is by far the most serious due to the ensuing massive release rate. During the Piper Alpha tragedy, for example, (Sylvester-Evans, 1991), FBR of the MCP-01 riser, although not the primary cause of the accident, resulted in the eventual collapse of the platform into the sea bed and the loss of 167 lives. The risk associated with FBR can be partly mitigated by using strategically positioned isolation valves placed along the pipeline. Nonetheless, an important part of the Safety Assessment Case (HMSO, 1992) requires that any such risk must be quantified and thereby controlled. Central to this task are the calculations of discharge rates and their variations with time during isolated and unisolated release.

In a previous publication (Mahgerefteh et al., 1997), we described the development of a mathematical model based on the Method of Characteristics (MOC) for predicting the dynamic response of emergency isolation valves and their ef-

Correspondence concerning this article should be addressed to H. Mahgerefteh.
Current address of P. Saha: Brown and Root Limited, Hill Park Court, Springfield Drive, Leatherhead, Surrey, KT22 7NL, U.K.

fect on the subsequent release rate following FBR. The responses of two types of commonly used valves were simulated. These included ball valves in which closure, normally fixed at a set rate, is initiated following sensing a drop in pressure and nonreturn or check valves that allow flow in one direction only.

Application of our simulations to FBR of a hypothetical rupture of a real North Sea pipeline revealed some dramatic differences in valve performance in isolating flow depending on a variety of factors such as pipeline length, valve proximity to the rupture plane, as well as flow reversal velocity. For example, by predicting the speed at which expansion waves propagate along the pipeline following FBR, we were able to show that a nonreturn check valve provides a faster response as compared to a ball valve only when the rupture plane happens to be in close proximity of the valve position. At large distances, however, the difference in performance becomes negligible. Also, short pipelines are much more prone to fluid induced oscillatory pressure transients following emergency isolation as compared to long pipelines. This type of phenomenon can either lead to momentary opening of a nonreturn valve due to cavitation (Simpson and Bergunt, 1996) or in some cases, resonance vibration of the pipeline (Koetzier, 1986).

Crucially, due to the complicated nature of the processes involved and the very long Central Process Unit (CPU) times, our study was confined to pipelines containing noncondensable gases only. It is inevitable that in a large majority of cases the quasi-adiabatic expansion process following FBR will result in significant fluid temperature drops, thereby causing the formation of a two-phase mixture. Also, many pipelines are used for the transport of flashing liquid hydrocarbons such as liquefied petroleum gas. The subsequent effects of the phase transition on valve performances are difficult to predict *a priori*.

In this article, we present the results of the application of an extension of our gas model (Mahgerefteh et al., 1997) to two-phase flows for simulating the effects of FBR on valve closure dynamics, and its subsequent influence on the discharge process and the pipeline integrity. The latter includes predictions of the resulting pressure surges brought about from having to bring the high velocity two-phase mixture to rest, as well as simulating the frequency and amplitude of the accompanying pressure oscillations. We highlight the subtle differences in behavior by simulating the FBR of the condensable gas mixture in the Piper Alpha MCP-01 riser (Cullen, 1990; Sylvester-Evans, 1991), and compare the results with those based on the assumption of permanent gas behavior. We use the data on the Piper Alpha accident as an example, as it is the only documented case relating to FBR of a relatively long pipeline for which actual field data have been recorded. An additional impetus for the present study is the temptation to ignore gas condensation effects during FBR in an attempt to avoid complexity and the very long CPU run times associated with simulating two-phase flows. The errors associated with such an approach are not known.

The consequences of not paying due consideration to the dynamic behavior of Emergency Shutdown Valves (ESDV) were graphically demonstrated only recently in a tragic accident (National Transportation Safety Board, 1994) in the U.S. involving the rupture of a 0.9 m dia pipeline. The resulting fire caused substantial damage to property. The pipeline operator's employees racing through the rush hour traffic to activate the pneumatically controlled valves arrived only to find that the pressure in the pipeline had diminished to the point that it was too low to operate the gas-power assisted motors on the valve closing mechanism. As a last resort, they attempted to close the nearest upstream valve through the 0.9 m pipe. However, the unequal pressures on either side of the gate made the valve, which took about 750 revolutions to close, increasingly difficult to turn. By the time the valve was closed, most of the inventory had been discharged.

In this study, the variations in pipeline fluid properties in the space-time domain are modeled by solving the pertinent conservation equations in conjunction with an equation of state (EoS) using an optimized version of the inverse marching method of characteristics or MOC (Mahgerefteh et al., 1999). We choose this method of solution as opposed to other numerical techniques such as finite difference (Chen et al., 1993, 1995; Bendiksen et al., 1991) and finite element methods (Lang, 1991; Bisgaard et al., 1987), as both have difficulty in handling the choking condition at the rupture plane. The MOC handles choked flow intrinsically via the Mach line characteristics. Moreover, MOC is considered to be more accurate than the finite difference method, as it is based on the characteristics of wave propagation. Hence, numerical diffusion associated with a finite difference approximation of partial derivatives is avoided (Chen et al., 1992). The effects of valve closure on the fluid dynamics within the pipeline during emergency shutdown are conveniently handled by specifying the appropriate boundary conditions across the valve at a selected point in the space-time grid. We dramatically reduce the very long CPU (such as 40 days on a 300 MHz Pentium II processor, which can be typical) which is synonymous with MOC by using second-order or curved characteristics (Flatt, 1986) coupled with a compound nested grid system. Here, the resolution of the numerical discretization is progressively reduced with the passage of time, and with distance from the rupture plane (Mahgerefteh et al., 1999; Saha, 1997).

Data relating to extensive validation of our FBR model against field measurements have been given elsewhere (Mahgerefteh et al., 1999). These include comparisons with the results of a series of pipeline FBR tests conducted by BP and Shell Oil on the Isle of Grain (Richardson and Saville, 1996a, b), as well as intact end pressure data relating to the MCP-01 riser rupture recorded during the night of the Piper Alpha tragedy (Sylvester-Evans, 1991). In the majority of cases, we obtain very good agreement between experiment and our numerical predictions.

Theory

MOC (Zucrow and Hoffman, 1976) involves replacing the appropriate conservation equations for an element of the fluid within the pipeline (see Appendix I) with the corresponding characteristics and compatibility equations and solving them numerically at selected space and time intervals along the pipeline.

In the case of unsteady generalized one-dimensional flow including heat transfer and friction, the characteristics equa-

tions are given by

$$\left(\frac{dt}{dx}\right)_p = \frac{1}{u} \quad \text{(Path line characteristic)} \tag{1}$$

$$\left(\frac{dt}{dx}\right)_{\pm} = \frac{1}{u \pm a} \quad \text{(Mach line characteristics)} \tag{2}$$

where a and U are, respectively, the sound and fluid velocities in the fluid at a given time t and distance x along the pipeline. Equations 1 and 2 stipulate the speed at which the expansion waves generated as a result of FBR propagate along the pipeline, and thereby control the corresponding fluid dynamics as a function of time. As such, they play a fundamental role is dictating the dynamic response of emergency shutdown valves.

The extremely rapid depressurization following FBR results in a nonlinear variation of fluid properties along the pipeline. This is particularly so for two-phase flows, or in the case of condensable gases, near the rupture plane where the transition from single- to two-phase flow is most pronounced. In our model we deal with these nonlinear variations by assuming curved characteristics where their curvature is accounted for by considering them as arcs of parabolas (Flatt, 1986). The loci of their intersections with the pipeline space and time grid discretization matrix are then calculated directly from solution of quadratic interpolation formulas in conjunction with the compatibility equations. We have already shown (Mahgerefteh et al., 1999) that the above, in conjunction with an especially developed fast mathematical algorithm, result in a considerable reduction in CPU, while at the same time, improving accuracy, as opposed to the commonly adapted assumption of linear characteristics (see, for example, Picard and Bishnoi, 1989).

The pathline compatibility C_o is

$$dP - a^2 d\rho = \frac{\psi}{u} dx = \psi dt \tag{3}$$

The positive C_+, and negative C_- compatibility equations can be written as

$$d_{\pm} P \pm \rho a d_{\pm} u = [\psi \pm a\beta] dt \tag{4}$$

The friction force term β is given by

$$\beta = -2\frac{f_w}{D}\rho u |u| \tag{5}$$

The flow-dependent wall friction factor f_w is obtained using the Moody approximation (Massey, 1983) to the Colebrooke equation. Gas and liquid viscosities required for the calculation of f_w are obtained according to the Ely and Hanley scheme for nonpolar gaseous mixtures, and the Dymond and Assael scheme for liquid mixtures (Massey, 1983).

The nonisentropic term ψ incorporating heat-transfer and frictional effects (Eq. 3) is given by

$$\psi = \varphi \frac{q_h - u\beta}{\rho T} \tag{6}$$

where q_h is the heat transfer from the pipe wall to the fluid. The thermodynamic function φ is given by

$$\varphi = \left(\frac{\partial P}{\partial s}\right)_{\rho} \tag{7}$$

It should be noted that in deriving Eqs. 3 and 4, we have ignored fluid/structure interactions by only considering rupture in straight, horizontal well anchored pipelines in which the fluid compressibility is by far smaller than the pipe wall elasticity (Tiley, 1989). We further assume thermodynamic and phase equilibrium in which the effect of slip between the two phases is ignored. The results of FBR experiments conducted by Shell Oil and British Petroleum on the Isle of Grain (Richardson and Saville, 1996a, b) have demonstrated the validity of this assumption for relatively long pipelines (> 100 m). As such, all hydrodynamic constitutive relations pertaining to momentum exchange between the two phases are nonexistent.

We employ the Peng-Robinson EoS (Peng and Robinson, 1976) for obtaining the appropriate thermodynamic and phase equilibrium data. This equation has been shown to be particularly applicable to high-pressure hydrocarbon mixtures (see, for example, de Reuck et al., 1996 and Assael et al., 1996). The number and the appropriate fluid phase(s) present at any given temperature and pressure on the other hand are determined using the stability test based on the Gibbs tangent plane criterion developed by Michelsen (Michelsen, 1982a, b, 1987). For unstable systems, the same technique also provides the composition of a new phase which can be split off to decrease the Gibbs energy of the mixture.

Pseudo-fluid properties for mixtures are calculated from the pure liquid and gas properties obtained from the EoS. The speed of sound a and φ (see Eq. 7) for real multicomponent single-phase fluids are obtained using standard expressions (see, for example, Picard and Bishnoi, 1987).

For two-phase flows, however, the analytical determinations of a and φ become complex. In this study these are evaluated numerically at a given temperature and pressure using the procedure described in a previous publication (Mahgerefteh et al., 1999).

The determination of the fluid temperature and, hence, other important properties such as density and pressure at a solution point (intersection of characteristics curves) requires the solution of the following equation

$$\rho_j - \rho\left(T_j^r, P_j\right) = 0 \tag{8}$$

The subscript j denotes conditions at the solution point, and the superscript r relates to the unknown temperature.

The solution of Eq. 8 becomes a root finding problem where a temperature is sought to match the density obtained from the compatibility equations to that calculated from an isothermal pressure-temperature flash.

This is achieved using the method of Brent (Brent, 1973; Press et al., 1994). It combines root bracketing, bisection, and inverse quadratic interpolation to converge from the neighborhood of a zero crossing. The bracketing of the root is performed by a routine which, given a function such as Eq. 8 and an initial guessed range for the root, expands the range

geometrically until a root is bracketed by the returned values (see the ZBRAC routine in Press et al., 1994). The above combines the robustness of bisection with the speed of a higher-order method when appropriate. Based on our experience of using this technique for FBR simulation, it produces rapid convergence.

Once the temperature is obtained at the solution point, the speed of sound and the parameter φ (Eq. 7) are found by a flash calculation.

The above steps are repeated until convergence for the dependent variables, P and ρ are achieved.

MOC is used to simulate the closure of check valves and ball valves by incorporating the appropriate boundary conditions at the downstream and upstream sides of each valve positioned at a chosen location on the discretization grid system. Full details of this procedure for a pipeline containing a permanent gas are given in a previous publication (Mahgerefteh et al., 1997).

In this study we essentially use the same methodology for simulating valve closure for pipelines containing two-phase or condensing gas mixtures with the exception of incorporating the relevant thermodynamic and hydrodynamic constituent equations described above for two-phase flows.

In the case of a check valve, we assume zero closure time whereas for a ball valve its closure rate is a required input parameter. We further assume the worse case scenario in which rupture takes place at the high-pressure end of the pipeline.

Results and Discussion

The following describes the results of a series of simulations relating to the FBR of the MCP-01 riser which actually took place during the night of the Piper Alpha tragedy (Cullen, 1990; Sylvester-Evans, 1991). The pipeline length and internal diameter were 54 km and 0.419 m, respectively. The inventory at the initial pressure and temperature of 117 bar and 283 K comprised (% mol); CH_4 (73.6), C_2H_6 (13.4), C_3H_8 (7.4), i-C_4H_{10} (0.4), n-C_4H_{10} (1.0), i-C_5H_{12} (0.08), n-C_5H_{12} (0.07), n-C_6H_{14} (0.02), N_2 (4.03). Under these conditions, the fluid is in the gaseous state. The heat-transfer coefficient and pipe roughness factor are taken as 5.0 W/m^{2}K and 0.04 mm, respectively. The latter is for carbon steel (Perry and Green, 1997). All simulations use a ''normal'' grid division of 500 m, which is progressively sub-divided into five sections over the last two elements near the rupture plane. This results in the last mesh closest to the rupture plane containing 25 grids, each 20 m in length. A time step of 0.103 s is used as stipulated by the Courant-Friedrich-Lewy stability criterion (Courant et al., 1952; Zucrow and Hoffman, 1976).

Fluid-phase behavior following FBR

The rapid depressurization at the rupture plane results in significant cooling of the gas. This in turn leads to the formation of a two-phase mixture, the front of which transverses from the rupture plane towards the closed end of the pipeline, eventually reverting to the gaseous state due to heat transfer from the pipeline walls. Figure 1 is a graphical presentation of this phenomenon. It shows the variation of the simulated volume fraction of liquid at the intact end of the pipeline

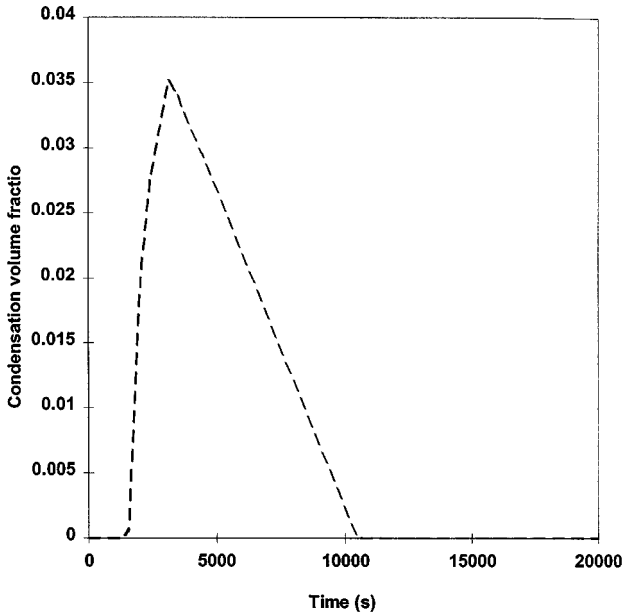

Figure 1. Variation of condensation volume fraction at closed end of pipeline with time.

with time following FBR. According to the data, it takes approximately 1,500 s for the front of the two-phase transition formed at the rupture plane to reach the intact end of the pipeline. This is immediately followed by a rapid and significant increase in the condensation volume fraction at this location peaking at 0.035 (about 15% w/w) at around 5,000 s following FBR. As the pipeline continues to depressurize, less inventory stays in the liquid phase and, at about 10,100 s following FBR, the intact end is once again exposed to gas only. The effects of the above processes on the dynamic behavior of isolation valves are investigated in the following.

Expansion wave velocity and depressurization profiles

The dynamic performances of both check valves and ball valves are primarily dictated by their activation times, t_a. This is the time lapsed between FBR and shutdown activation. For a check valve, t_a is dictated by its location relative to the position of flow reversal. In the case of a ball valve set to trigger at a pre-specified pressure on the other hand, t_a is essentially controlled by the rate of depressurization within the pipeline. Both these phenomena are influenced directly by the speed of expansion waves generated as a result of FBR propagating through the fluid medium away from the rupture plane.

Figure 2 shows predicted expansion wave velocity profiles over the first 360 m of pipeline as measured from the rupture plane. The expansion wave velocity is the velocity of the fluid relative to the speed of sound as given by the right running Mach line ($= u + a$). Curves A and B respectively show the results at 0 and 0.6 s following FBR on the basis of real fluid behavior, whereas curves C and D show the corresponding data where gaseous condensation is ignored. The formation of the two-phase mixture at the rupture plane results in a sudden drop in sound velocity and, hence, the observed

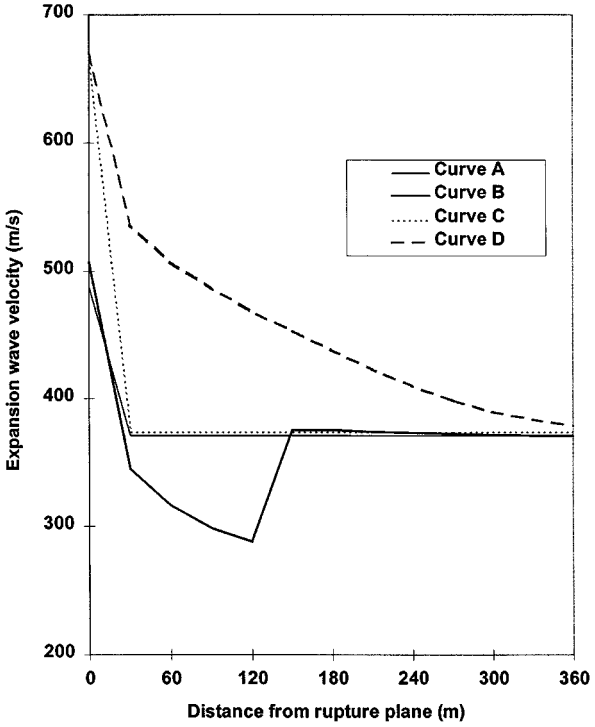

Figure 2. Expansion wave velocity at different time intervals over the first 360 m of pipeline as measured from the rupture plane.

Curve A: Two-phase; $t = 0$ s following FBR; Curve B: Two-phase; $t = 0.6$ s following FBR; Curve C: Gas; $t = 0$ s following FBR; Curve D: Gas; $t = 0.6$ s following FBR.

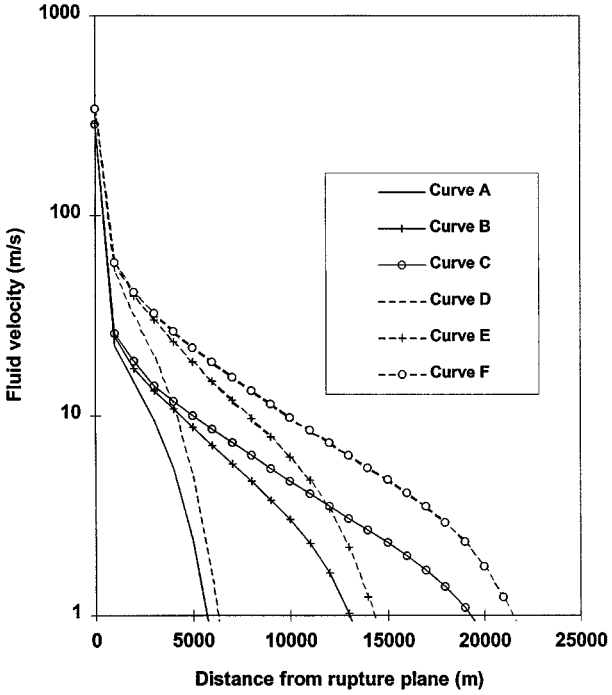

Figure 3. Variation of fluid velocity with distance from the rupture plane at different time subsequent to FBR.

Curve A: Condensable gas; $t = 9.23$ s; Curve B: Condensable gas; $t = 27.69$ s; Curve C: Condensable gas; $t = 46.15$ s; Curve D: Permanent gas; $t = 9.23$ s; Curve E: Permanent gas; $t = 27.69$ s; Curve F: Permanent gas; $t = 46.15$ s.

marked reduction in the expansion wave velocity as compared to a permanent gas.

At $t = 0$ s, this effect is only noticed at the rupture plane (cf. curves A and C), because the two-phase transition interface has not moved beyond this position. At $t = 0.6$ s, however, the phase transition interface has traveled about 120 m (curve B) from the rupture plane towards the intact end of the pipeline. Over this distance, the presence of a two-phase mixture results in a relatively large difference in expansion wave velocities (curves B and D). The subsequent sharp rise in expansion wave velocity at 120 m (curve B) corresponds to the point in the pipeline where only gas phase exists, and, hence, in this region and beyond, the difference in behavior between the two models is less pronounced.

Clearly, the condensation of the gas mixture will reduce valve activation time and, hence, cause a delay in emergency isolation. The data in Figure 3 showing the variation of fluid velocity with distance from the rupture plane at different time intervals following FBR quantify this effect. Curves A–C, respectively, show the results for the condensable gas at 9.23, 27.69, and 46.15 s following FBR. Curves D–F on the other hand show the corresponding data for the permanent gas. The reduction in expansion wave velocity due to condensation is manifested in slowing down of the discharge process thus leading to an inevitable delay in the valve activation time. Considering a check valve placed 6.1 km from the rupture plane as an example, the activation time in conjunction with the two-phase mixture is ca. 9.20 s as compared to ca. 7.6 s for the permanent gas. These are obtained by determining the times corresponding to zero flow velocity at the given valve location. Even such a small difference in activation time represents a massive difference in the amount of inventory released prior to complete pipeline isolation. The effect becomes even more pronounced with increasing distance between the check valve and the rupture plane.

Figure 4 shows the variation of pressure with distance from the rupture plane at different times following FBR. Curves A–C show the results for the condensable gas at 9.23, 27.69 and 46.15 s, respectively, whereas curves D–F show the corresponding data based on permanent gas assumption. These profiles are necessary for determining ball valve activation times.

The permanent gas model gives rise to larger pressure drops leading to faster depressurization rate predictions as compared to those based on the condensable gas mixture. These differences become more pronounced with the passage of time. For example, in the case of a ball valve placed at a distance of 6.1 km from the rupture plane and set to initiate shutdown on sensing a pressure drop of 10 bara below the normal working pressure (117 bar), the corresponding activation times depending on permanent gas or two-phases fluid are 27.7 s and 32 s, respectively. Once again, the difference in activation times predicted for the two cases becomes more noticeable when the proximity of the valve is further from the rupture plane.

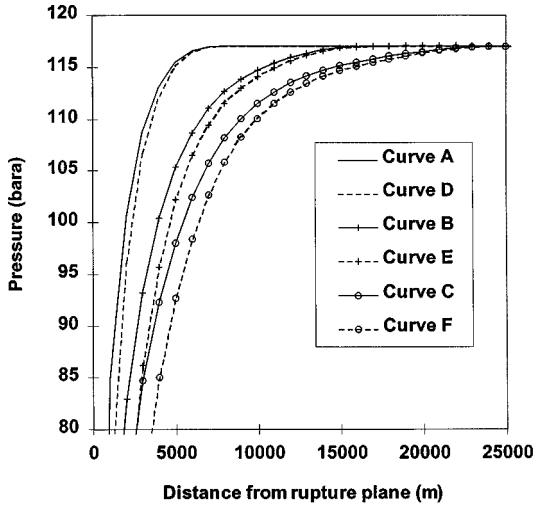

Figure 4. Variation of pressure with distance from the rupture plane at different times subsequent to FBR.

Curve A: Two-phase; $t = 9.23$ s; Curve B: Two-phase; $t = 27.69$ s; Curve C: Two-phase; $t = 46.15$ s; Curve D: Permanent gas; $t = 9.23$ s; Curve E: Permanent gas; $t = 27.69$ s; Curve F: Permanent gas; $t = 46.15$ s.

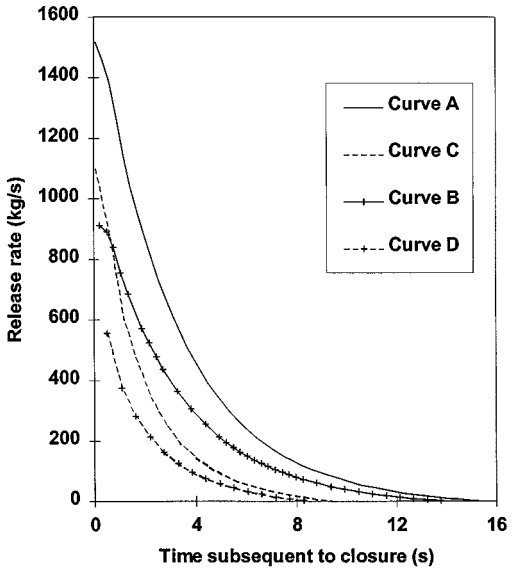

Figure 5. Variation of release rate with time subsequent to check valve closure for various arbitrary delays in valve shutdown.

Curve A: Two-phase; valve closure delay after passage of flow reversal = 1.37 s; Curve B: Two-phase; valve closure delay after passage of flow reversal = 6.47 s; Curve C: Permanent gas; valve closure delay after passage of flow reversal = 1.37 s; Curve D: Permanent gas; valve closure delay after passage of flow reversal = 6.47 s.

Mass release data

The general trends observed in conjunction with the permanent gas are found to be applicable for two-phase or condensable flows. Namely, a check valve offers a better degree of protection in terms of limiting the amount of escaped inventory prior to pipeline isolation as compared to a ball valve only when either is placed in close proximity to the rupture plane. At long distances, the difference in performance becomes insignificant. However, considerable differences in discharge rates are obtainable depending on the fluid state.

Figure 5 shows the variation of release rate at the rupture plane with time subsequent to valve closure for various arbitrary delays in shutdown for a check valve placed 300 m from the rupture plane. Such time delays may be necessary in practice in order to avoid valve damage due to ''slamming'' (see, for example, Thorley (1989) and Lee et al. (1992)). Curves A and B, respectively, show the results in conjunction with the condensable mixture for valve shutdown taking place 1.37 s and 6.47 s after the passage of flow reversal. Curves C and D show the corresponding results on the basis of permanent gas behavior.

It is clear from the data that the predicted release rates in the case of condensable gas mixture are significantly higher than those for the permanent gas following emergency isolation of the pipeline. Pipeline depressurization times are also longer. For example, in the case of a 1.37 s delay in shutdown, complete evacuation of the isolated section of the pipeline takes ca. 10 s (curve C) for the permanent gas as compared to ca. 16 s (curve A) in the case of a two-phase mixture. Similar differences can be observed for a closure delay of 6.47 s.

The combination of the higher flow rate and the slower depressurization rate for the two-phase mixture clearly indicates that the total inventory released prior to pipeline isolation will be greater than that for the gas pipeline. For the ranges tested, this is regardless of the delay in valve closure.

Pressure-time history

Figure 6 shows the effect of time delay on valve closure following the passage of flow reversal on the pressure-time history at the upstream side of a check valve placed 300 m from the rupture plane. Curves A–D show the data for the condensable gas mixture, whereas curves E–H relate to the permanent gas.

As expected, when the valve shuts immediately upon sensing the flow reversal (zero time delay), no pressure oscillation is predicted by either model (curves A and E). At larger time delays, the pressure buildup on the upstream side of the valve increases dramatically and the subsequent oscillations resulting from the reflections of the high-pressure fluid off the face of the check valve and the intact end of the pipeline become more pronounced.

The upstream pressure in conjunction with the condensable mixture is always larger than that for the permanent gas; the difference becomes more pronounced with the delay in valve closure. The latter is due to the increase in the volume fraction of liquid with the passage of time prior to valve closure.

The magnitude of the observed pressure peaks shown in Figure 6 are, however, alarming. For example, a delay of only 6.47 s in valve closure following the passage of flow reversal results in a relatively rapid pressure rise of almost 30 bara on the upstream side of the valve. This may in practice give rise to serious consequences by undermining pipeline or valve structural integrity.

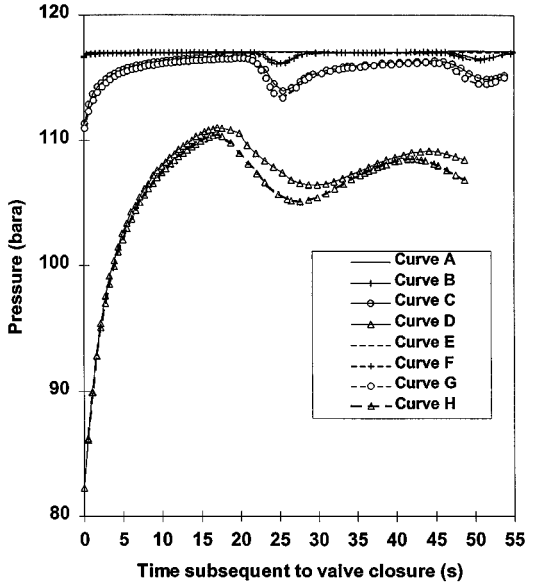

Figure 6. Effect of time delay in valve closure following the passage of flow reversal on the pressure-time history at the upstream side of a check valve placed 300 m from the rupture plane.

Curve A: Two-phase; time delay = 0 s; Curve B: Two-phase; time delay = 0.57 s; Curve C: Two-phase; time delay = 1.37 s; Curve D: Two-phase; time delay = 6.47 s; Curve E: Permanent gas; time delay = 0 s; Curve F: Permanent gas; time delay = 0.57 s; Curve G: Permanent gas; time delay = 1.37 s; Curve H: Permanent gas; time-delay = 6.47 s.

Figure 7 shows the upstream ball valve pressure-time histories for different closure rates. Curves A and B show the two-phase data for closure rates of 2.54 and 5.08 cm/s, respectively, whereas curves C and D show the corresponding data for the permanent gas. As before, the valve is assumed to activate on sensing a pressure drop of 10 bara below the normal operating pressure.

As expected, both models show that the faster is the valve closure rate, the greater is the accrual of line pressure. The closure times after activation for closure rates of 2.54 cm/s and 5.08 cm/s are 16.5 s and 8.25 s, respectively.

Interestingly, both models give rise to similar trends of substantially equal magnitude. As the valve starts to close, the upstream pressure continues to drop for as long as the aperture diameter is still comparable to that of the pipe. On approaching the halfway stage of closure, the pressure then starts to build with the two-phase model predicting a slightly higher pressure than the permanent gas. This is followed by a constant pressure region when the valve is completely shut.

Figure 8 shows the corresponding pressure variation with time at the downstream side of the closing ball valve. In this case, there is a significant difference in behavior between the permanent gas and the condensable gas mixture with the latter giving rise to a much slower depressurization rate. This is because the rapid expansion brought about as a result of flow through the closing valve leads to the evaporation of the liquid fraction into the vapor phase. Subsequently, the pressure drop across the closing valve is much smaller for the evaporating two-phase mixture as compared to a permanent gas.

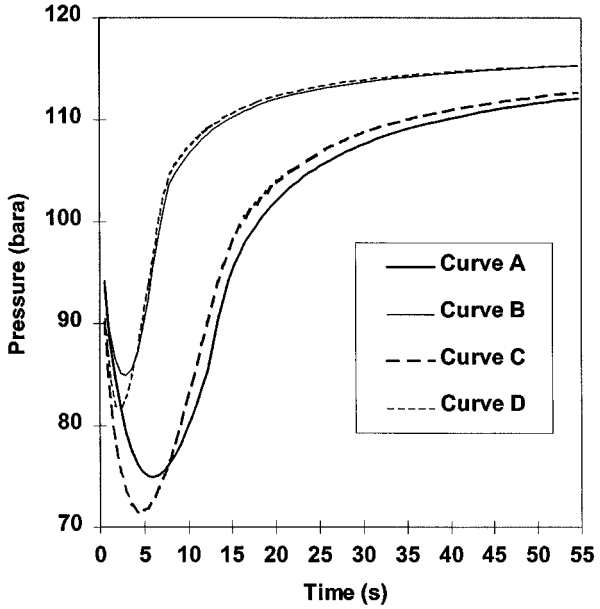

Figure 7. Upstream pressure-time histories at the downstream side of a closing ball valve for different closure rates.

Curve A: Two-phase, 2.54 cm/s; Curve B: Two-phase, 5.08 cm/s; Curve C: Permanent gas, 2.54 cm/s; Curve D: Permanent gas, 5.08 cm/s.

Pressure surge data

Figure 9 shows the variation of pressure surge on the upstream face of the check valve vs. delay in time for complete

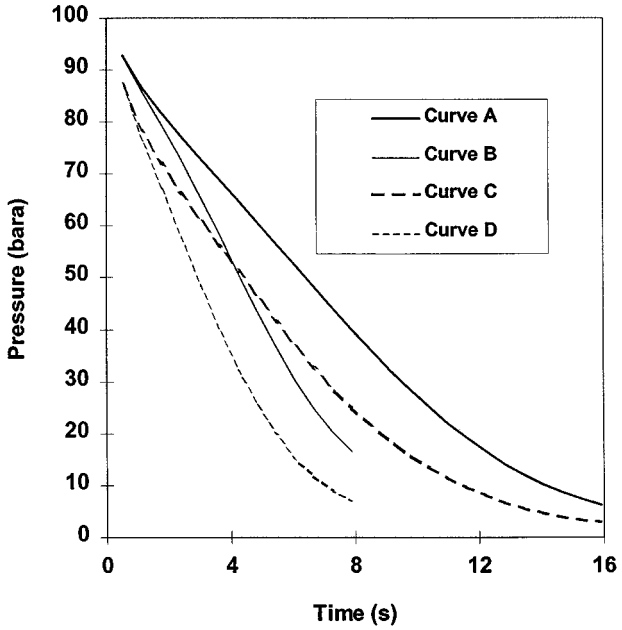

Figure 8. Downstream pressure-time histories at the downstream side of a closing ball valve for different closure rates.

Curve A: Two-phase, 2.54 cm/s; Curve B: Two-phase, 5.08 cm/s; Curve C: Permanent gas, 2.54 cm/s; Curve D: Permanent gas, 5.08 cm/s.

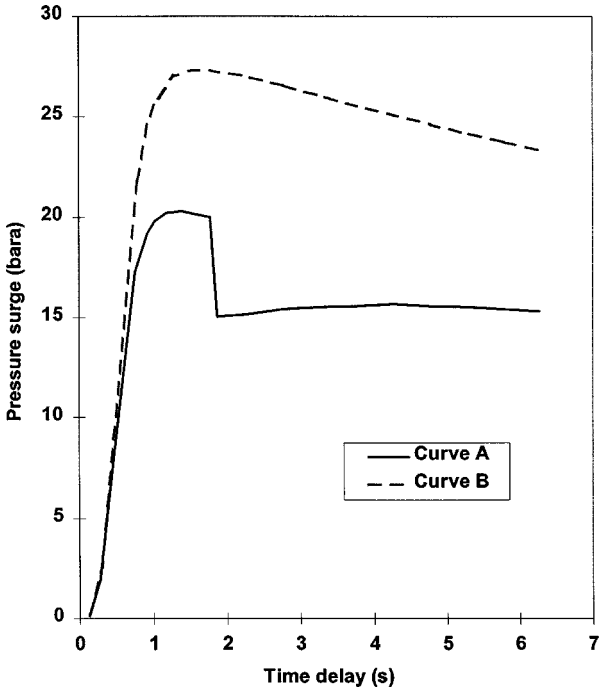

Figure 9. Variation of pressure surge at various check valve closure time delays following the passage of flow reversal.

Curve A: two-phase; Curve B: permanent gas.

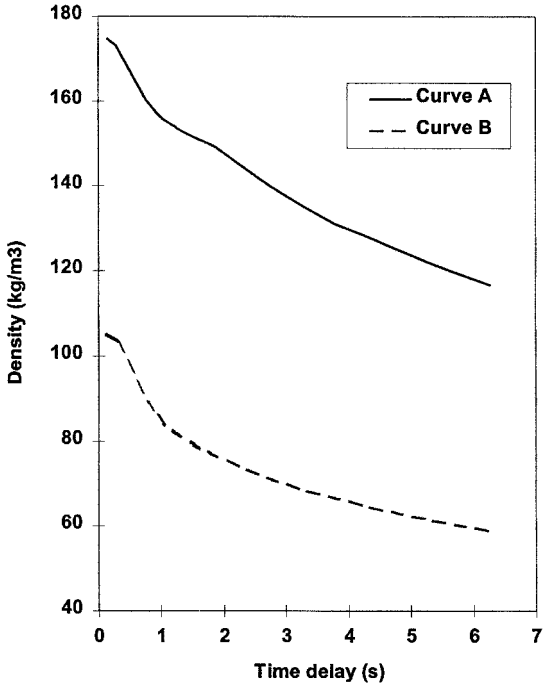

Figure 10. Variation of upstream fluid density at valve location with various closure time delays subsequent to the passage of flow reversal.

Curve A: two-phase; Curve B: permanent gas.

valve closure following the passage of flow reversal. Curve A shows the data for the condensable gas, whereas curve B shows the corresponding data for the permanent gas. Pressure surge data were calculated using the Joukowski (1900) correlation, given by

$$\Delta P = \rho\left(au_r + u_r^2\right) \tag{9}$$

where ΔP is the pressure surge.

U_r is the flow reversal velocity at the time of complete valve closure. Three important observations may be made on the basis of the data shown in Figure 9.

(a) As expected, no pressure surge is observed when the valve closes instantaneously, upon the passage of flow reversal. However, a delay in closure results in a rapid increase in the pressure surge reaching a peak value up to a closure delay of about 1 s. Longer delays in valve closure results in a reduction in the pressure surge. The latter is in response to the progressively smaller amount of fluid remaining in the isolable section of the pipeline following valve closure.

(b) The discontinuity in the pressure surge data in the case of the real fluid (curve A) is due to the phase transition.

(c) Surprisingly, a higher pressure surge is observed in the case of the permanent gas as opposed to the condensable mixture despite its higher density. The data in Figure 10 showing the corresponding variation of fluid density at the valve location with closure time delay confirm the latter.

The lower pressure surge observed in the case of the two-phase mixture is due to the overriding effect of the terms U_r^2 in Eq. 9. Figure 11 shows the variation of square of the flow

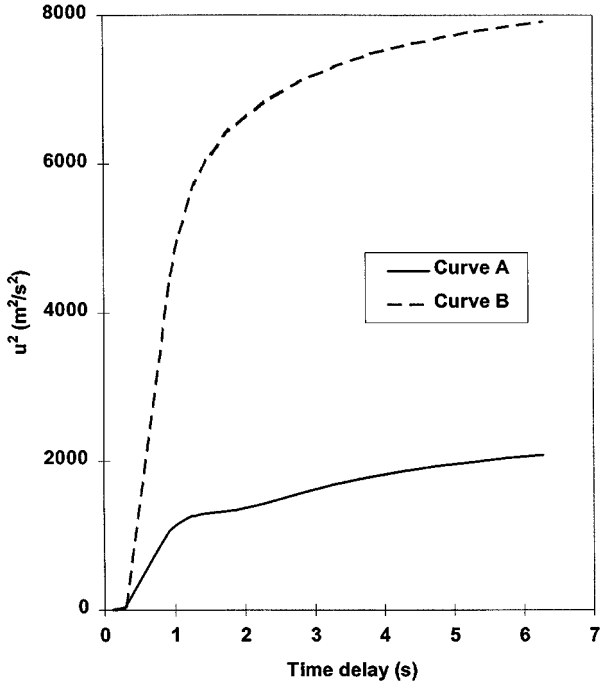

Figure 11. Variation of the square of the flow reversal velocity at the valve location with various closure time delays subsequent to the passage of flow reversal.

Curve A: two-phase; Curve B: permanent gas.

reversal velocity vs. delay in valve closure following the passage of flow reversal for both fluid systems. As it is clear, formation of liquid in the case of the condensable gas mixture (curve A) slows down the flow reversal velocity due to larger frictional force effects as compared to a gas. The net effect is a substantial reduction in the pressure surge.

Conclusion

The response of emergency shutdown valves following FBR is critically controlled by the subsequent variations in the fluid dynamics within the pipeline. The results of our study show that the state of the fluid inside the pipeline during the depressurization process plays an important role in this event.

In essence, a transition into the two-phase region results in three important effects, two of which are detrimental in terms of increasing the risks involved.

The first is the slowing down of expansion waves propagating from the rupture plane towards the intact end of the pipeline. As these waves are in effect the sole messengers of FBR to the rest of the pipeline, any delay in their transmission will lead to a subsequent delay in ESDV activation times. The result is a greater amount of inventory released prior to pipeline isolation. This effect becomes more pronounced when the position of the EDSV is further relative to the rupture plane.

The second effect, and equally detrimental as the first, is the increased mass release rate. This is simply a consequence of the higher density of the two-phase mixture as compared to that of the gas.

The third, and, perhaps, the most controversial, is in fact beneficial in terms of protecting valve and pipeline integrity by leading to a significant reduction in pressure surge following emergency isolation. This is primarily a consequence of the more important effect of the velocity of the escaping fluid as compared to its density in governing the magnitude of the resulting pressure surge. Despite leading to a higher density, the presence of liquid in the two-phase mixture also results in a substantial reduction in flow velocity due to increased frictional forces. The net effect is a smaller pressure surge as compared to gas. A useful byproduct of the greater frictional effects is a faster dying out of the pressure wave oscillations set up within the isolated section of the pipeline following emergency shutdown.

In conclusion, this article highlights the importance of studying, in a quantitative manner, the variations in the fluid dynamics along the pipeline when simulating the dynamic behavior of emergency shutdown valves following FBR. The simplification of the process by assuming permanent gas behavior can be entirely inappropriate in cases where the escaping fluid may undergo a phase transition.

At present, we find no evidence of valve dynamic simulation receiving the important considerations that it merits in practice. We strongly believe that in view of the Piper Alpha tragedy, this type of study should form an integral part of the Safety Assessment Case for all pipelines transporting significant amounts of inventory.

The Method of Characteristics adopted in this study, coupled with an appropriate thermodynamic and phase equilibrium package has proven to be a powerful and robust tool for carrying out such detailed analysis. The only drawback is still the comparatively long CPUs. The advent of faster computers coupled with the development of more efficient mathematical algorithms are expected to play a major role in addressing this issue.

Literature Cited

Assael, M. J., J. P. Martin Trusler, and T. Tsolakis, *Thermophysical Properties of Fluids*, Imperial College Press, London (1996).

Barlas, S., ''Pipeline Safety Law Reauthorisation,'' *Pipeline and Gas J.*, **226**, 6 (April 1999).

Bendiksen, K. H., D. Malnes, R. Moe, and S. Nuland, ''The Dynamic Two-Fluid Model OLGA: Theory and Application,'' *SPE Production Eng.*, 171 (May 1991).

Bisgaard, C., H. H. Sorensen, and S. Spangenberg, ''A Finite Element Method for Transient Compressible Flow in Pipelines,'' *Int. J. Num. Meth. Fluids*, **7**, 291 (1987).

Bond, J., ''IChemE Accidents Database,'' IChemE, Rugby (1996).

Brent, R. P., *Algorithms for Minimisation Without Derivatives*, Prentice Hall, Englewood Cliffs, NJ (1973).

Chen, J. R., S. M. Richardson, and G. Saville, ''A Simplified Numerical Method for Transient Two-Phase Flow,'' *Trans. I. Chem. E.*, **71A**, 304 (1993).

Chen, J. R., S. M. Richardson, and G. Saville, ''Numerical Simulation of Full-Bore Ruptures of Pipelines Containing Perfect Gases,'' *Trans. Inst. Chem. Eng. Part B*, **70**, 59 (1992).

Chen, J. R., S. M. Richardson, and G. Saville, ''Modelling of Two-Phase Blowdown from Pipelines: I. A. Hyperbolic Model Based on Variational Principles,'' *Chem. Eng. Sci.*, **50**, 695 (1995).

Courant, R. E., M. Isaacson, and M. Reeves, ''On the Solution of Non-Linear Hyperbolic Differential Equations by Finite Differences,'' *Comm. on Pure and Appl. Math.*, **5**, 243 (1952).

Cullen, W. D., ''The Public Inquiry into the Piper Alpha Disaster,'' Dept. of Energy, HMSO, London (1990).

deReuck, K. M., R. J. B. Craven and A. E. Elhassan, *Transport Properties of Fluids: Their Correlation, Prediction and Estimation*, J. Millat, J. H. Dymond and C. A. Nieto de Castro, eds., IUPAC, Cambridge Univ. Press, Cambridge (1996).

Flatt, R., ''Unsteady Compressible Flow in Long Pipelines Following a Rupture,'' *Int. J. Num. Meth. Fluids*, **6**, 83 (1986).

HMSO, *A Guide to Offshore Installation* (*Safety Case*) *Regulations*, Health and Safety Executive, Bootle, U.K. (1992).

Hovey, D. J., and E. J. Farmer, ''Pipeline Accident, Failure Probability Determined from Historical Data,'' *Oil and Gas J.*, 104 (July 1993).

Joukowski, N. E., ''Uber den Hydraulischer Stoss in Vanserieitungsrohren,'' *Memoires de l'Academic Imperiale de Sciences*, St. Petersburg, 8 Ser., **9**, 5 (1900).

Koetzier, H., ''Dynamic Behaviour of Large Non-Return Valves,'' paper H4, 213, 5*th Int. Conf. on Pressure Surge*, Hanover, Germany (1986).

Lang, E., ''Gas Flow in Pipelines Following a Rupture Computed by a Spectral Method,'' *J. Appl. Math. and Physics* (*ZAMP*), **42**, 183 (1991).

Lee, C. L., A. T. Jocson, and S. T. Hsu, *Unsteady Flow and Fluid Transients*, D. Bettess and L. Watts, eds., Balkema pub., London, p. 365 (1992).

Mahgerefteh, H., P. Saha, and I. G. Economou, ''A Study of the Dynamic Response of Emergency Shutdown Valves Following Full Bore Rupture of Gas Pipelines,'' *Trans. Inst. Chem. Eng., Part B*, **75**, 201 (1997).

Mahgerefteh, H., P. Saha, and I. G. Economou, ''Fast Numerical Simulation for Full Bore Rupture of Pressurized Pipelines,'' *AIChE J.*, **45**, 1191 (1999).

Massey, B. S., *Mechanics of Fluids*, Van Nostrand Reinhold, Wokingham, U.K. (1983).

Michelsen, M. L., ''Multi-Phase Isenthalpic and Isentropic Flash Algorithms,'' *Fluid Phase Equil.*, **33**, 13 (1987).

Michelsen, M. L., ''The Isothermal Flash Problem: I. Stability,'' *Fluid Phase Equil.*, **9**, 1 (1982a).

Michelsen, M. L., ''The Isothermal Flash Problem: II. Phase-Split Calculation,'' *Fluid Phase Equil.*, **9**, 21 (1982b).

Montiel, H., J. A. Vilchez, J. Arnaldos, and J. Casal, ''Pipeline Rupture,'' *J. Hazard. Mater*., **51**, 77 (1996).
National Transportation Safety Board, ''Pipeline Accident Report: Texas Eastern Transportation National Gas Pipeline Explosion and Fire,'' Document number PB95-916501, National Transportation Safety Board, Edison, NJ (Jan. 18, 1995).
Peng, D. Y., and D. B. Robinson, ''A New Two-Constant Equation of State,'' *Ind. Eng. Chem. Fund.* **15**, 59 (1976).
Perry, R. H., and D. W. Green, *Perry's Chemical Engineering Handbook*, 7th ed., McGraw Hill, London (1997).
Picard, D. J., and P. R. Bishnoi, ''The Calculation of the Thermodynamic Sound Velocity in Two-Phase Multi-Component Fluids,'' *Int. J. Multiphase Flow*, **13**, 295 (1987).
Picard, D. J., and P. R. Bishnoi, ''The Importance of Real-Fluid Behaviour in Predicting Release Rates Resulting from High Pressure Sour-Gas Pipeline Ruptures,'' *Can. J. Chem. Eng*., **67**, 3 (1989).
Picard, D. J., and P. R. Bishnoi, ''The Importance of Real-Fluid Behaviour and Non-Isentropic Effects in Modelling Decompression Characteristics of Pipeline Fluids for Application in Ductile Fracture Propagation Analysis,'' *Can. J. Chem. Eng*., **66**, 3 (1988).
Richardson, S. M., and G. Saville, ''Isle of Grain Pipeline Depressurisation Tests,'' HSE OTH 94441, HSE Books, HSE, Bootle, U.K. (1996a).
Richardson, S. M., and G. Saville, ''Blowdown of LPG Pipelines,'' *Trans. Inst. Chem. Eng*., *Part B*, **74**, 235 (1996b).
Press, H. W., S. A. Teukolsky, W. T. Vetterling, and B. P. Flannery, *Numerical Recipes in Fortran*, 2nd ed., Cambridge Univ. Press, Cambridge, U.K. (1994).
Saha, P., ''Modelling the Dynamic Response of Emergency Shutdown Valves Following Full Bore Rupture of Long Pipelines,'' PhD Thesis, Univ. College London, London, U.K. (1997).
Simpson, A. R., and A. Bergant, ''Interesting Lessons from Column Separation Experiments,'' *Proc. Int. Conf. on Pressure Surges and Fluid Transients in Pipelines and Open Channels*, A. Boldy, ed., BHR Group Conference Series, No. 19 (1996).
Sylvester-Evans, R., ''Background to the Piper Alpha Tragedy,'' *Trans. Inst. Chem. Eng*., **69B**, 3 (1991).
Thorley, A. R. D., ''Check Valve Behaviour Under Transient Flow Conditions: A State-of-the-Art-Review,'' *Trans. of the ASME, J. of Fluids Engineering*, **111**, 178 (1989).
Tiley, C. H., ''Pressure Transients in a Ruptured Gas Pipeline with Friction and Thermal Effects Included,'' PhD Thesis, City Univ., London, U.K. (1989).
U.S. Department of Transport, ''Transportation of Hazardous Liquids by Pipeline,'' Accident Report Data Base Code of Federation Regulations (CFR), Title 49D, Part 195 (1982–1997).
Zucrow, M. J., and J. D. Hoffman, *Gas Dynamics*, Vols. I and II, Wiley, New York (1976).

Appendix: Characteristics and Compatibility Equations

The pertinent continuity, momentum, and energy conservation equations for an element of the fluid within the pipeline are, respectively, given by Zucrow and Hoffman (1976)

$$\rho_t + \rho u_x + u\rho_x = 0$$

$$\rho u_t + \rho u u_x + P_x - \beta = 0$$

$$P_t + uP_x - a^2(\rho_t + u\rho_x) - \psi = 0$$

where ρ, u, P, β, and a are the density, velocity, pressure, friction force term, and acoustic velocity of the fluid, respectively. Subscript t and x denote property derivative with respect to time and space (in the x-direction), respectively.

Manuscript received May 21, 1999, and revision received Nov. 23, 1999.